Kidney Diseases

Research Article

Kidney Dis 2025;11:320–331
DOI: 10.1159/000545851

Received: December 18, 2024
Accepted: March 30, 2025
Published online: April 14, 2025

The Effect of Low-Density Lipoprotein Receptor-Related Protein-1 on Acute Kidney Injury and Renal Tubular Epithelial Triglyceride Accumulation

Weiteng Wang[a, b] Jieyi Luo[b, c] Yingwen Chen[a, b] Huaban Liang[b]
Zhilian Li[b] Yuanhan Chen[a, b] Jintao He[a, b] Xinling Liang[a, b]

[a]School of Medicine, South China University of Technology, Guangzhou, China; [b]Department of Nephrology, Guangdong Provincial People's Hospital (Guangdong Academy of Medical Sciences), Southern Medical University, Guangzhou, China; [c]Guangdong Cardiovascular Institute, Guangdong Provincial People's Hospital, Guangdong Academy of Medicial Sciences, Guangzhou, China

Keywords
Acute kidney injury · Low-density lipoprotein receptor-related protein-1 · Triglycerides · Apoptosis · Receptor-associated protein

Abstract
Introduction: Various types of acute kidney injury (AKI) are associated with triglyceride (TG) accumulation in renal tubular epithelial cells, but the role and mechanisms of TG accumulation in AKI remain unclear. This study aimed to explore the impact of low-density lipoprotein (LDL) receptor-related protein-1 (LRP1), a protein that mediates TG endocytosis, on ischemia-reperfusion injury (IRI)-induced AKI and TG accumulation in renal tubular epithelial cells. ***Methods:*** We established an IRI-induced AKI mouse model and assessed LRP1 expression by Western blot, RT-qPCR, and immunofluorescence. The LRP1 antagonist receptor-associated protein (RAP) was used to evaluate the effect of LRP1 on AKI and renal TG accumulation in the AKI mouse model. We applied a carbonyl cyanide 3-chlorophenylhydrazone (CCCP)-induced hypoxia-reoxygenation model to HK-2 cells in vitro. The effects of very low-density lipoproteins (VLDLs) and LRP1 silencing on TG levels, cell viability, and apoptosis in HK-2 cells were observed. ***Results:*** We observed significant TG accumulation in renal tissue during IRI-AKI, accompanied by upregulation of LRP1 in renal tubular epithelial cells. After intervention with the LRP1 antagonist RAP, AKI was significantly alleviated, and TG levels in renal tissue were notably reduced. However, in the in vitro model, although VLDL increased TG levels in HK-2 cells in both normal culture and hypoxia-reoxygenation conditions, it did not alleviate the decrease in cell viability induced by CCCP. In the absence of exogenous VLDL, silencing LRP1 still reduced CCCP-induced TG accumulation and cell apoptosis, although the reduction in TG levels was less pronounced compared to the presence of exogenous VLDL. ***Conclusion:*** Our study demonstrated that the increased expression of LRP1 on renal tubular epithelial cells contributes to IRI-induced AKI and TG accumulation. The injury effects of LRP1 on the renal tubules are independent of TG endocytosis. Targeting the inhibition of LRP1 may emerge as a novel therapeutic strategy for AKI.

karger@karger.com
www.karger.com/kdd

Correspondence to:
Xinling Liang, xinlingliang_ggh@163.com

Introduction

Acute kidney injury (AKI) is a clinical syndrome characterized by rapid deterioration of kidney function and abrupt kidney damage. AKI is widely prevalent across the globe. More than 20% of patients experience AKI during hospitalization [1]. The mechanisms of AKI remain incompletely elucidate. Currently, several pathophysiological or metabolic processes have been shown to be involved in AKI, such as renal tubular epithelial cell injury, immune-mediated inflammation and microcirculatory disturbances [2–4].

Previous researches have found renal tissues excessive lipid accumulation in AKI, including triglyceride (TG), cholesterol, sphingolipid and fatty acid [5–7]. TG serves as a major form of energy storage, primarily stored in adipose tissue [8]. TGs are primarily transported in circulation in the form of chylomicrons and very low-density lipoproteins (VLDLs) [9]. Under physiological conditions, TGs cannot directly enter renal tubular epithelial cells but instead enter indirectly in the form of lipoprotein degradation products (fatty acids and glycerol) [10]. TGs accumulation in renal tubular epithelial cells has been reported in cisplatin, Lipopolysaccharide and ischemia-reperfusion injury (IRI)-mediated AKI [11, 12]. In addition, several studies showed that TG levels of tubular epithelial cells increase following endotoxic, toxic, and ischemic injury in vitro [13]. These findings suggested that abnormal TG metabolism in renal tubular epithelial cells might be involved in AKI. However the effect of accumulation of TG on AKI and the mechanisms of TG accumulation in renal tubular epithelial cells remain inadequately explored.

We performed a proteomic analysis of the renal cortex in a renal IRI model and observed significant increase of low-density lipoprotein (LDL) receptor-related protein-1 (LRP1). As a cellular membrane-localized receptor, LRP1 not only mediates the endocytosis of macromolecular proteins, including lipoproteins, but also plays a role in signal transduction, such as the mitogen-activated protein kinase pathway [14–16]. Although previous studies have shown that LPR1 mediates the effects of TG endocytosis by interacting with apoE-enriched chylomicrons and VLDL, the effect of LRP1 on renal TG accumulation and AKI remains unclear. In the present study, we explored the potential effect of LRP1 on AKI and renal tubular epithelial cells TG accumulation.

Methods

Animal Experimental Protocol

Male C57BL/6 mice, aged 6–8 weeks and weighing 20–25 g, were acquired from the Guangdong Medical Animal Laboratory Center. The mice were housed in a controlled specific-pathogen-free environment, with a temperature of 23 ± 2°C and relative humidity of 55 ± 5%. The animal room was kept on a 12-h light/12-h dark cycle. All mice were administered a standard diet and water. The animal study received formal approval from the Animal Ethics and Welfare Committee of Guangdong Provincial People's Hospital (KY2024-159-01).

Experimental mice were randomly allocated into distinct groups: sham-operated group (sham), renal ischemia–reperfusion injury group (IRI) and IRI with receptor-associated protein (RAP) group (IRI + RAP). The IRI-AKI animal model was constructed by following the protocol of our previous study [17]. In brief, renal ischemia was induced by occluding the bilateral renal pedicles with vascular clamps for 30 min, followed by reperfusion for 2 days. Before IRI procedure, a 100 μL dose of 50 nM receptor-associated protein (Cat No. HY-P76479A, MedChemExpress, NJ, USA) was administered via intravenous injections (IV) to inhibit LRP1 function [18].

Assessment of Kidney Pathology

Kidney sections (3–4 μm) were stained with periodic acid-Schiff (PAS) to evaluate renal injury. We calculated the tubular injury score by quantifying specific histopathological alterations, including vacuolar deformation of tubular epithelial cells, loss of the brush border, tubular dilation, cast formation and cell lysis. Injury severity was assessed using a scoring system from 0 to 4 determined as follows: no injury, 0; 25% injury, 1; 50% injury, 2; 75% injury, 3; 100% injury, 4 [19]. We randomly selected 6 fields of view in each section under the microscope (×200) to calculate an average injury score. The modified Oil Red O Staining Kit (Cat. No. C0158M, Beyotime, Shanghai, China) was used to evaluate the content and distribution of neutral lipids in tissues according to the manufacturer's manual provided.

Evaluation of Renal Function

Serum creatinine (Scr) and blood urea nitrogen (BUN) were assessed by the QuantiChrom™ Creatinine Assay Kit (Cat. No. DICA-500, BioAssay Systems, CA, USA) and QuantiChrom™ Urea Assay Kit (Cat. No. DIUR-100, BioAssay Systems, CA, USA) in accordance with the manufacturer's specifications.

Cell Cultivation and Experimental Interventions

HK-2 cells were cultured in DMEM/F12 (Lot. No. 10092016, Gibco, Thermo Fisher Scientific, Waltham, USA) with the addition of 10% fetal bovine serum (Cat.

No. 164210, Procell Life Science & Technology, Wuhan, China) at 37°C with 5% CO_2. To mimic the injury of renal tubular epithelial cells caused by ischemia-reperfusion in vitro, HK-2 cells were incubated for 4 h in glucose-free Krebs-Ringer bicarbonate buffer supplemented with 15 μM carbonyl cyanide 3-chlorophenylhydrazone (CCCP) (HY-100941, MedChemExpress, NJ, USA) at normoxic conditions at 37°C [20]. Post-treatment, cells were recovered for 2 h in complete DMEM/F12 medium supplemented with 10% fetal bovine serum. In vitro, we added VLDL (Cat. No. 20617ES05, Yeasen Biotechnology, Shanghai, China) at varying concentration gradients from 50 μg/mL to 400 μg/mL to culture medium after 4 h of ATP depletion induced by CCCP to examine whether TG exert damaging influence on cells. To knock down LRP1 expression, HK-2 cells were transfected with 50 nM LRP1 (human) small interfering RNA (siRNA) (No. JY20240607GYQ-SI01, Hanbio Biotechnology, Shanghai, China) and Lipofectamine 2000 (TL201-01, Vazyme Biotech, Nanjing, China) for 6 h.

Western Blot Analysis

HK-2 cells and kidney tissues samples were lysed using RIPA lysis buffer (Beyotime) supplemented with protease inhibitor, phenylmethylsulfonyl fluoride. Subsequently, equivalent quantities of proteins were separated by SDS-PAGE on 4–20% gradient gels and transferred onto 0.45 μm PVDF membranes (No. IPVH00010, Millipore, Billerica, MA, USA). After PBS washing, membranes were blocked with 5% nonfat dried skimmed milk in TBS-Tween for 1 h at room temperature, then incubated overnight at 4°C with primary antibodies. Finally, the membranes were incubated with secondary antibody for 1 h before detection at room temperature. The relevant antibodies are as follows: anti-cleaved caspase-3 (1:1,000, #9661, Cell Signaling Technology, Danvers, MA, USA), anti-caspase-3 (1:1,000, #9662, Cell Signaling Technology, Danvers, MA, USA), anti-GAPDH (1:5,000; No. 60004-1-IG; Proteintech, Wuhan, China), and anti-LRP1(1:200; Cat. No. ab92544; Abcam, Cambridge, UK); Horseradish peroxidase-conjugated goat anti-rabbit (1:5,000; Cell Signaling Technology, Danvers, MA, USA), Horseradish peroxidase-conjugated goat anti-mouse (1:5,000; Cell Signaling Technology, Danvers, MA, USA), and donkey anti-goat (1:5,000; Proteintech, Wuhan, China). The membranes were detected with Image LAS 500. Band intensities were quantified using ImageJ software, and we use SPSS Statistics version 26.0 to perform statistical analyses.

RNA Isolation and Quantitative Polymerase Chain Reaction (RT-qPCR)

Total RNA was isolated from kidney tissues and cell samples using TRIzol reagent and subsequently reverse-transcribed into complementary DNA using a PrimeScript RT Reagent Kit (Cat. RR037A, Takara, Japan). Quantitative PCR analysis was conducted using the SYBR Green PCR Master Mix (Cat. RR820A, Takara, Wuhan, Japan). Gene expression levels were quantified using the $2^{-\Delta\Delta Cq}$ method, with GAPDH serving as the normalized control. The primer sequences used in the real-time RT-PCR are shown in Table 1.

Immunofluorescence Staining

The frozen sections stored at −80°C need first to be returned to room temperature. Frozen tissue sections were fixed in 4% paraformaldehyde for 10 min and permeabilized with 0.5% Triton X-100 for 10 min. After blocking with 5% bovine serum albumin for 30 min at room temperature, the sections were incubated with anti-LRP1 (1:200; Cat. No. ab92544; Abcam, Cambridge, MA, USA). Following washing three times in PBS, the frozen sections were incubated with Alexa Fluor 555-conjugated goat anti-rabbit (1:500; #4413; Cell Signaling Technology, Danvers, MA, USA) secondary antibodies for 1 h. To label proximal tubules, the sections were incubated with lotus tetragonolobus lectin (LTL; 1:500; Cat. No. FL-1321; Vector Laboratories, Newark, CA, USA) for 30 min. To label the nuclei, mounting medium containing DAPI was used to perform covering the slide, and images were captured using a Nikon AX confocal microscope within 7 days.

Proteomics Analysis

After homogenizing kidney tissue with liquid nitrogen, trypsin (V5111, Promega, Germany) was added to prepare samples suitable for mass spectrometry analysis. The samples were subjected to LC-MS/MS analysis using an LTQ Orbitrap mass spectrometer (Thermo Scientific, San Jose, CA, USA) equipped with an Eksigent nanoLC system (Eksigent Technologies, LLC, Dublin, CA, USA). The mass spectrometry data were processed using MaxQuant (v1.6.15.0). The search parameters were set as follows: the database used was Mus_musculus_10090 SP 20201214.fasta (17,063 sequences), with a decoy database included to calculate the false discovery rate due to random matches. The enzyme specificity was set to Trypsin/P, allowing up to two missed cleavage sites. The minimum peptide length was set to seven amino acid residues, and the maximum number of modifications per peptide was set to five. The precursor ion mass

Table 1. Sequences of primers for quantitative RT-PCR

Gene	Primer sequence
Lrp1 (mouse)	Forward: 5′- ACT ATG GAT GCC CCT AAA ACT TG-3′ Reverse: 5′- GCA ATC TCT TTC ACC GTC ACA -3′
GAPDH (mouse)	Forward: 5′- AGG TCG GTG TGA ACG GAT TTG-3′ Reverse: 5′- TGT AGA CCA TGT AGT TGA GGT CA-3′
Lrp1 (human)	Forward: 5′- CTA TCG ACG CCC CTA AGA CTT-3′ Reverse: 5′- CAT CGC TGG GCC TTT ACT CT-3′
GAPDH (human)	Forward: 5′- GTC TCC TCT GAC TTC AAC AGC G-3′ Reverse: 5′- ACC ACC CTG TTG CTG TAG CCA A-3′

RT-qPCR, reverse transcription-quantitative polymerase chain reaction.

tolerance for both the first search and main search was set to 20 ppm, and the fragment ion mass tolerance was set to 20 ppm. Carbamidomethylation of cysteine was set as a fixed modification, while oxidation of methionine and N-terminal acetylation of proteins were set as variable modifications. The false discovery rate for both protein identification and peptide-spectrum match identification was maintained at 1%. We identified proteins related to TG metabolism through comparison in the KEGG database.

Cell Viability Assay

Cell viability was determined using the Enhanced Cell Counting Kit-8 (Cat. No. C0042, Beyotime, Shanghai, China) according to the manufacturer's instructions. The cell viability was calculated as a percentage of the absorbance in the treated group relative to the control group.

Flow Cytometric Analysis

Apoptosis levels of cells were assessed using a fluorescein isothiocyanate Annexin V apoptosis detection kit (No. KGA1102, Keygen Biotech, Jiangsu, China) in accordance with the manufacturer's instructions. The medium was collected, followed by washing the cells with cold PBS, collecting the PBS wash as well. The adherent cells were then digested with 0.25% EDTA-free trypsin. Following centrifugation, the cells were washed twice with pre-cooled PBS and resuspended in 500 μL binding buffer. Then, cell suspension was transferred to a flow cytometry tube, and 5 μL each of fluorescein isothiocyanate Annexin V and propidium iodide (PI) were added. At room temperature, the mixture was incubated in the dark for 5 min. Then, we use flow cytometry with CytoFLEX Flow Cytometer (Beckman, USA) to analyze apoptosis within 1 h using FlowJo, version 10.8.1.

Lipid Detection

A specific quantity of tissues was weighed to prepare the homogenate, and then TG Content Assay Kit (Cat. No. BC0625, Solarbio, Beijing, China), Amplex Red Cholesterol and Cholesteryl Ester Assay Kit (Cat. No. S0211M, Beyotime, Shanghai, China), and Free Fatty Acids (FFAs) Content Assay Kit (Cat. No. BC0595, Solarbio, Beijing, China) were used to assess the content of lipids in tissues according to the instructions provided. Triglyceride Assay Kit (Cat. No. S03027, Rayto, Shenzhen, China) was used to measure the blood lipids based on the instructions given.

Statistical Analysis

All experimental data were presented as mean ± SEM and were analyzed using SPSS statistical software, version 26.0. One-way analysis of variance was employed for multiple group comparisons, and least significant difference method was used between pairwise comparisons. Student's *t* tests were used to evaluate differences between two groups. The $p < 0.05$ was considered statistically significant.

Results

TG Accumulation in the Animal Model of AKI

We established the mouse AKI model by Bi-IRI operation. The renal tissue pathology showed significant necrosis and detachment of renal tubular epithelial cells in mice with Bi-IRI (Fig. 1a). The acute tubular injury score in the IRI group was significantly higher than sham-operated mice (Fig. 1b). The levels of Scr and BUN were markedly elevated after IRI compared to those of sham-operated mice (Fig. 1c, d). Oil Red O staining showed that IRI induced neutral lipid accumulation in the renal

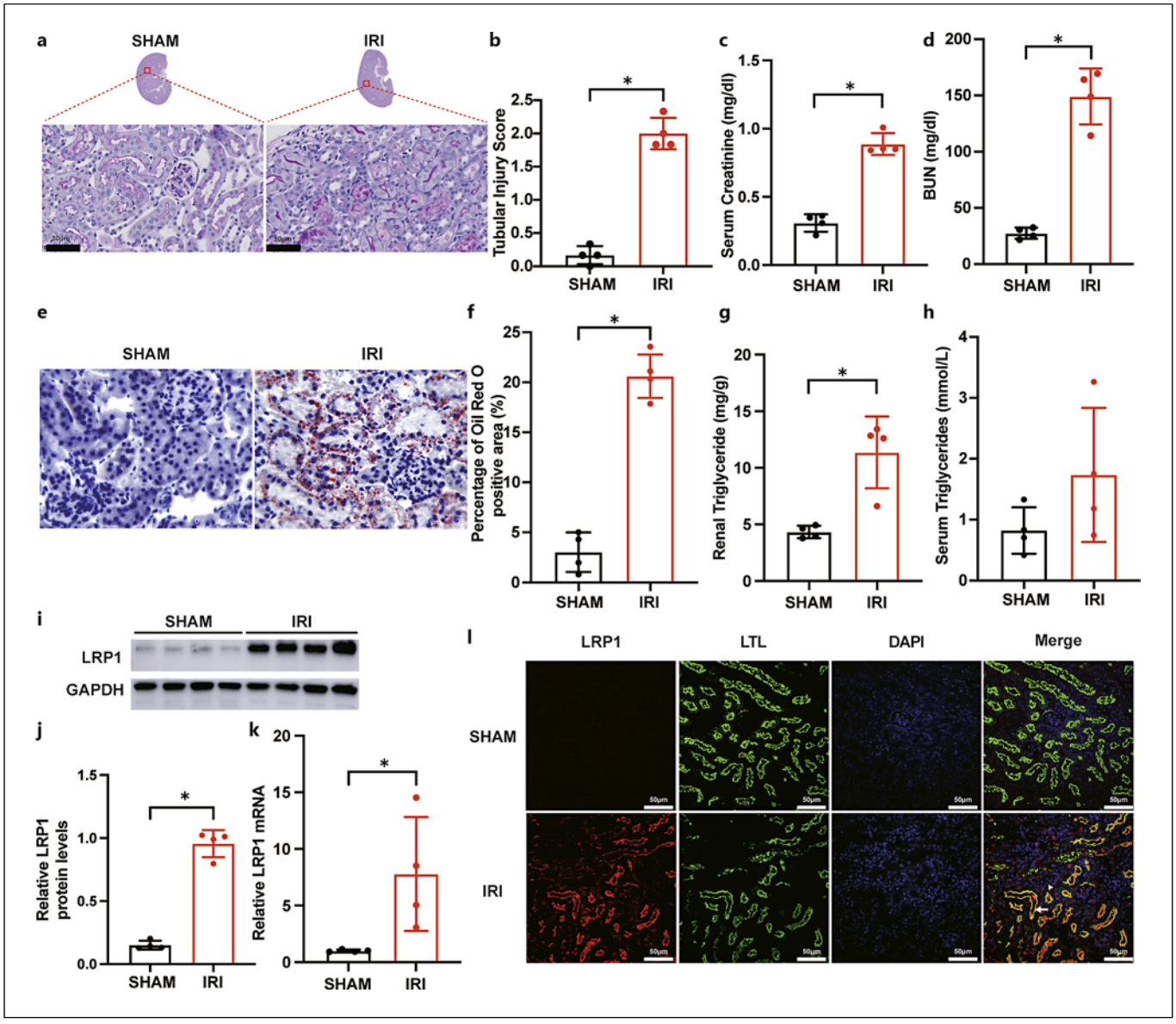

Fig. 1. Triglyceride accumulation in the renal tissue of AKI animal model. **a** PAS staining showed obviously renal tubular epithelial cell injury in the IRI group (200×). **b** Quantification of tubular injury. Serum creatinine (**c**) and BUN (**d**) elevated in the IRI models. **e**, **f** Oil Red O staining showed neutral lipid accumulation in renal tubules in IRI group (400×). Renal triglycerides (**g**) and serum triglycerides (**h**) were measured in the sham-operated and IRI mice. **i**, **j** Western blot was conducted to assess the protein levels of LRP1. **k** qPCR was used to detect the mRNA level of LRP1. **l** Immunostaining for LRP1 (red), LTL (green), and DAPI (blue) was used in frozen renal sections from sham-operated and IRI mice (200×). *$p < 0.05$. White arrow indicates LRP1 expression at the brush border of proximal tubules; white triangle indicates LRP1 expression at the basolateral side of proximal renal tubular epithelial cells. BUN, blood urea nitrogen; LRP1, low-density lipoprotein receptor-related protein-1; IRI, ischemia-reperfusion injury; LTL, lotus tetragonolobus lectin.

tubular epithelial cells (RTECs) (Fig. 1e, f). We detected TG levels of renal cortex tissue and found that TG accumulation was evident in the IRI group (Fig. 1g). However, IRI did not significantly alter the serum TG levels (Fig. 1h).

LRP1 Was Markedly Increased in the Animal Model of AKI

The mechanisms underlying TG accumulation in IRI-AKI were unclear. We performed a proteomic analysis of renal cortex in renal IRI model and observed changes in TG

Table 2. Proteins associated with triglyceride metabolism identified through proteomics

Protein	IRI/Con ratio	FDR-adjusted *p* value
LPL	0.35	<0.001
LRP1	2.25	<0.001
LRPAP1	0.61	<0.001
GPAM	0.67	<0.001
AGPAT2	1.84	<0.001
GK	0.60	<0.001

IRI, ischemia-reperfusion injury; FDR, false discovery rate; LPL, lipoprotein lipase; LRP1, low-density lipoprotein receptor-related protein-1; LRPAP1, low-density lipoprotein receptor-related protein-associated protein 1; GPAM, glycerol-3-phosphate acyltransferase mitochondrial; Agpat2, 1-acylglycerol-3-phosphate O-acyltransferase 2; GK, glycerol kinase.

metabolism-related proteins including lipoprotein lipase (LPL), LRP1, LDL receptor-related protein-associated protein 1, glycerol-3-phosphate acyltransferase mitochondrial, 1-acylglycerol-3-phosphate O-acyltransferase 2, and glycerol kinase (Table 2; online suppl. Table 1; for all online suppl. material, see https://doi.org/10.1159/000545851). Among these proteins, LRP1, which mediates TG and cholesterol endocytosis by binding with VLDL, is the most significantly upregulated protein. Whereas LPL is the most significantly downregulated protein. LPL mediates the hydrolysis of TG to generate FFA and glycerol [21]. However, neither inhibition nor activation of LPL improved the severity of IRI-AKI (online suppl. Fig. 1). Therefore, our subsequent research focused on LRP1. Western blot confirmed the higher expression of LRP1 in the IRI group compared to the sham group (Fig. 1i, j). Consistently, RT-qPCR results indicated an upregulation of LRP1 transcripts after IRI (Fig. 1k). Immunofluorescence analysis showed that LRP1 was barely expressed in renal tubular epithelial cells of the sham-operated mice. In the renal tissues of the IRI group mice, LRP1 expression was markedly increased in both the brush border and the basolateral side of LTL-positive renal tubular epithelial cells. This suggested that IRI induced the upregulation of LRP1 in proximal renal tubular epithelial cells (Fig. 1l).

LRP1 Antagonists Alleviated Renal Tubular Injury in the Mouse Model of AKI

Next, we explored the role of LRP1 in IRI-AKI and the impact of LRP1 on TG accumulation. Considering that RAP is a well-established antagonist of LRP1, we used RAP to interfere with LRP1's function [22, 23]. At the histopathologic level, RAP treatment markedly reduced tubular injury (Fig. 2a, b). RAP administration also resulted in a significant improvement in renal function compared to the untreated IRI group (Fig. 2c, d). Oil Red O staining indicates that RAP alleviates the accumulation of neutral lipids in RTECs induced by IRI (Fig. 2e, f). Furthermore, RAP reduced TG and free fatty acid levels in the renal cortex (Fig. 2h, j). Serum TG and renal tissue cholesteryl ester were not significantly decreased by RAP (Fig. 2g, i). RAP neither affected expression nor transcription levels of LRP1, consistent with the mechanism by which RAP antagonizes LRP1 (Fig. 2k–n). These results indicated LRP1 might play an injury role in IRI-AKI and mediate renal TG accumulation.

LRP1 Upregulated in HK-2 Cells following ATP Depletion

To simulate IRI in renal tubular epithelial cell in vitro, HK-2 cells were treated with CCCP and neutral buffer to induce ATP depletion, followed by reperfusion with serum-containing medium. Microscopic examination revealed that HK-2 cells treated with CCCP underwent significant morphological alterations, including cell shrinkage, irregular shape formation, reduced adhesion, partial detachment from the culture surface, and the presence of intracellular vacuoles (Fig. 3a). The CCK-8 assay demonstrated HK-2 cell viability significant decrease after CCCP treatment (Fig. 3b). Western blot analysis showed increased levels of cleaved caspase-3 following ATP depletion and upregulated LRP1 expression compared to the control group (Fig. 3c–g).

Knockdown of LRP1 Reduced IRI-Induced Apoptosis in HK-2 Cells Independent on Inhibiting TG Endocytosis

To explore the role of TG in the pathogenesis of AKI, we used different concentration gradients of VLDL, the lipoprotein containing a high level of TG, to evaluate the effect of TG on HK-2 cell survival. We found that various concentration gradients of VLDL had no effect on HK-2 cell death after ATP depletion (Fig. 4a). We further knocked down LRP1 using siRNA to investigate whether LRP1 could mediate tubular epithelial cells IRI and TG endocytosis. RT-qPCR and Western blot analysis confirmed a significant reduction in LRP1 protein levels following siRNA treatment (Fig. 4b–d). SiRNA-LRP1-1 was used in subsequent experiments to knock down LRP1. The addition of VLDL to the normally cultured or ATP depletion HK-2 cells both increased the levels of TG and FFA (Fig. 4e, f). Regardless of the presence of

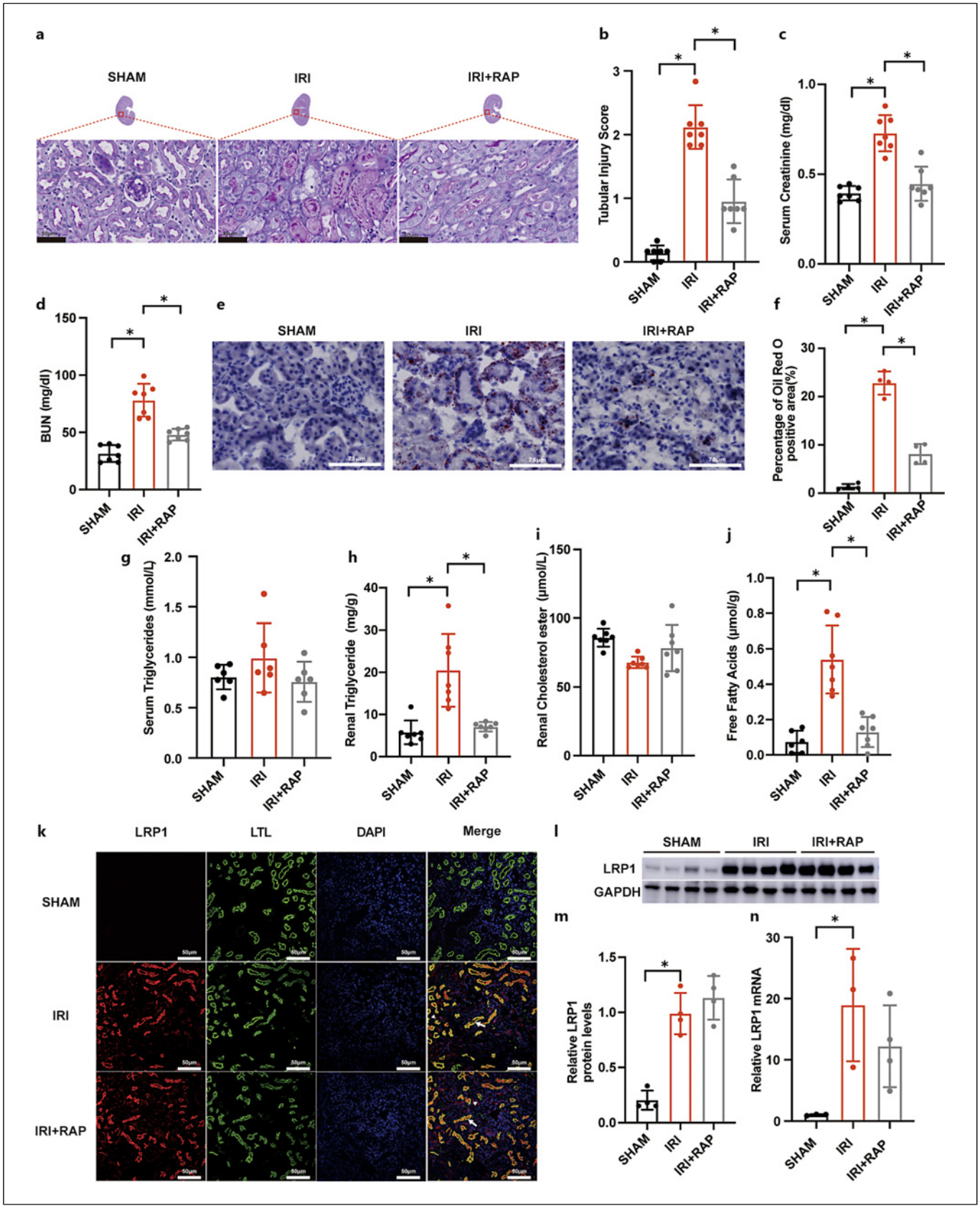

2

(For legend see next page.)

exogenous VLDL, silencing LRP1 could alleviate the increased level of TG induced by ATP depletion. However, in the presence of exogenous VLDL, LRP1 knockdown reduced TG more pronouncedly (Fig. 4e, f). Western blot analysis showed a decrease in cleaved caspase-3 levels in the LRP1 knockdown group compared to the Scramble group (Fig. 4g, h). Knocking down LRP1 reversed the decrease in HK-2 cell viability caused by IRI (Fig. 4i). Flow cytometry analysis similarly showed that LRP1 knockdown significantly reduced the proportion of Annexin-positive cells in this ischemia-reperfusion cell model (Fig. 4j, k). These results demonstrated that LRP1 mediate IRI in renal tubular epithelial cells but may not through TG endocytosis.

Discussion

In this study, we found that LRP1, which is located on the cell membrane and mediates the endocytosis of TG-rich lipoproteins, is upregulated in tubular epithelial cells [24]. Furthermore, antagonizing LRP1 in IRI-induced

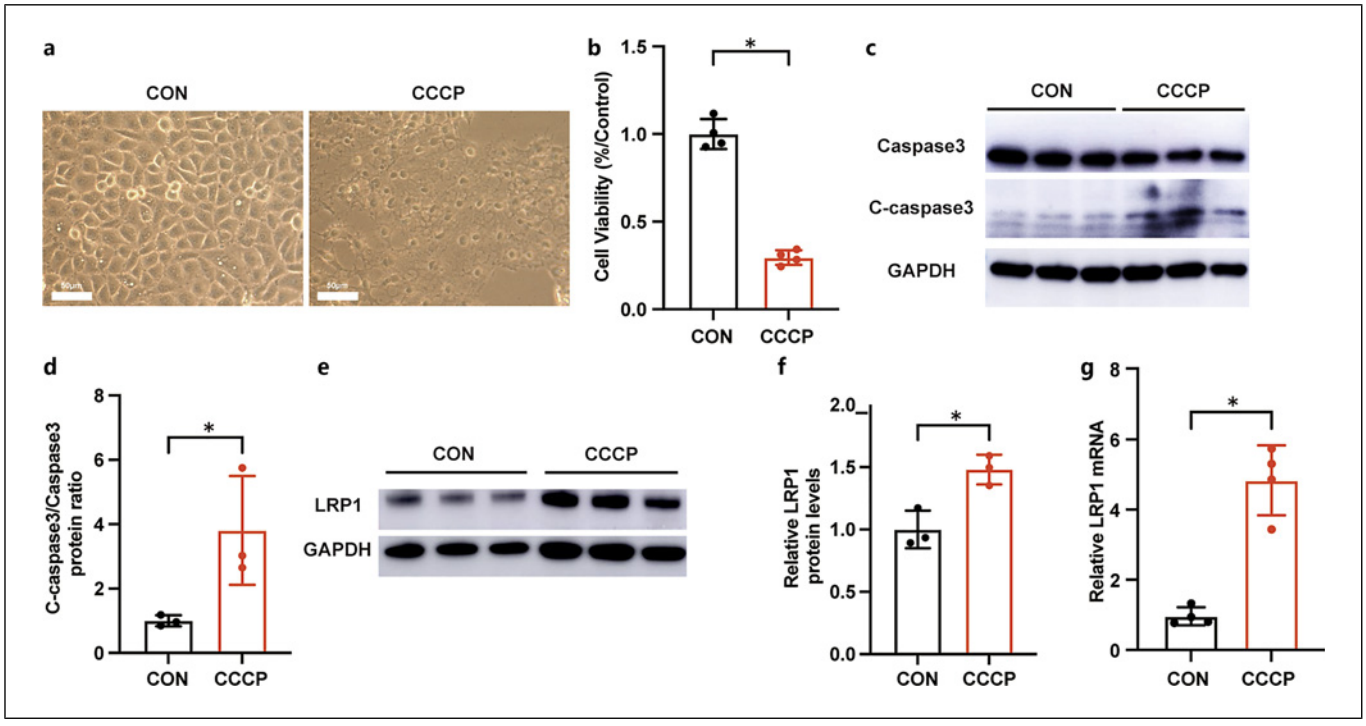

Fig. 3. LRP1 increased in the CCCP-induced cellular ATP depletion model. HK-2 cells were treated with 15 μM CCCP for 4 h and followed by 2 h reoxygenation. **a** Observation of cell morphology under a light microscope. **b** CCK-8 assay to assess cell viability in the CON and CCCP groups. **c**, **d** Western blot analysis of caspase-3 and cleaved caspase-3 expression in HK-2 cells. **e**, **f** Western blot analysis of the expression of LRP1 in HK-2 cells. **g** qPCR was used to detect the mRNA level of LRP1 in HK-2 cells. *$p < 0.05$. CCCP, carbonyl cyanide 3-chlorophenylhydrazone; LRP1, low-density lipoprotein receptor-related protein-1; C-caspase-3, cleaved caspase-3.

Fig. 2. RAP improved IRI induced AKI and reduced renal triglyceride accumulation. **a** PAS staining showed RAP improved renal tubular epithelial cell injury (200×). **b** Quantification of tubular injury in each group. Serum creatinine (**c**) and BUN (**d**) levels were measured in each group. **e**, **f** Oil Red O staining showed RAP reduce neutral lipid accumulation in renal tubules (400×). **g** Serum triglyceride was measured in each group. Measurement of renal cortex triglycerides (**h**), cholesterol ester (**i**), and renal cortex FFA (**j**) in each group. **k** immunostaining for LRP1(red), LTL(green), and DAPI (blue) was used in frozen renal sections in each group (200×). **l**, **m** Western blot was conducted to assess the protein levels of LRP1. **n** qPCR was used to detect the mRNA level of LRP1. *$p < 0.05$. White arrow indicates LRP1 expression at the brush border of proximal tubules; white triangle indicates LRP1 expression at the basolateral side of proximal renal tubular epithelial cells. BUN, blood urea nitrogen; LRP1, low-density lipoprotein receptor-related protein-1; FFA, free fatty acid; IRI, ischemia-reperfusion injury; LTL, lotus tetragonolobus lectin; RAP, receptor-associated protein.

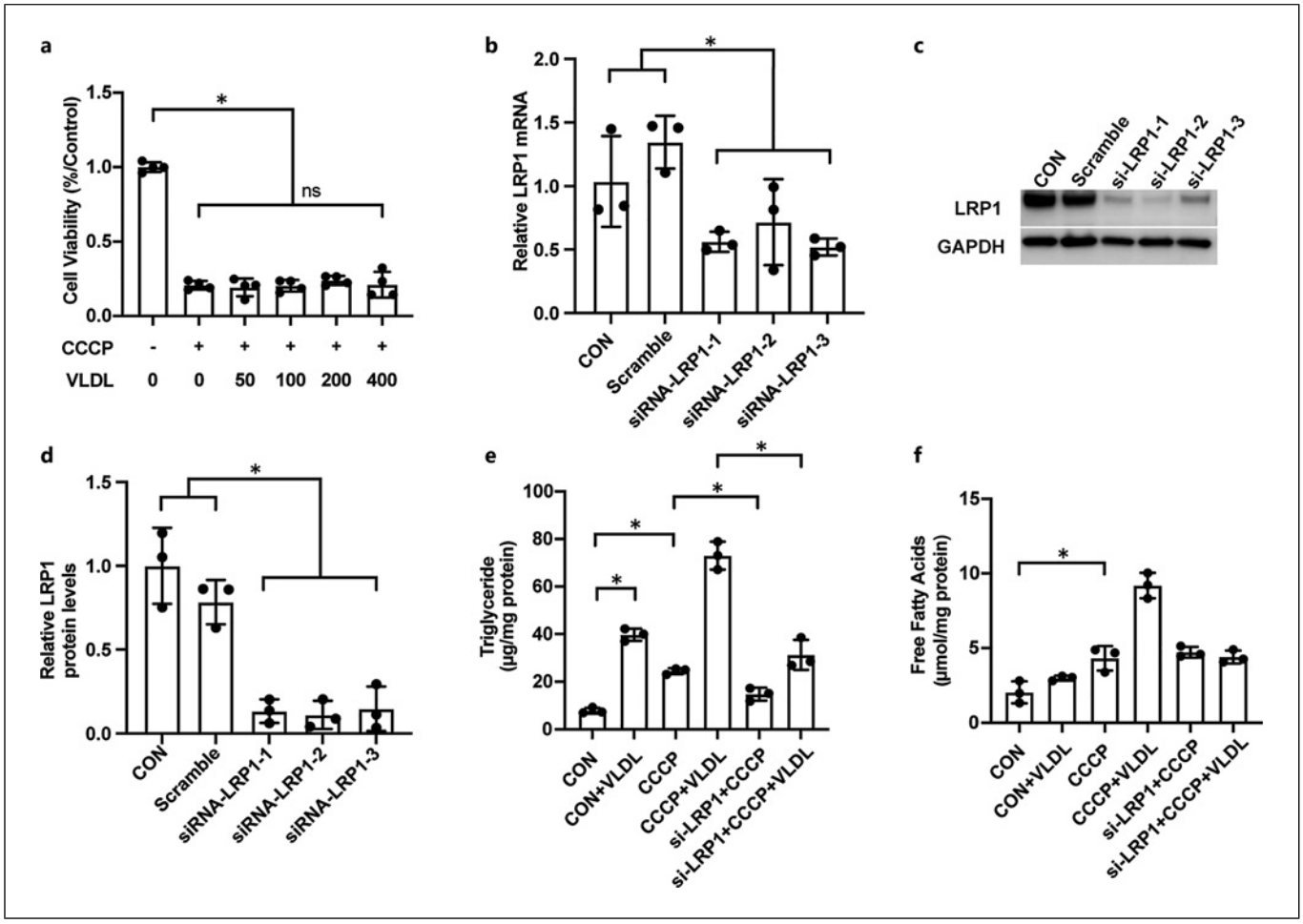

4

(Figure continued on next page.)

AKI animal models reduced TG accumulation in the renal cortex and improved renal function. Similarly, in the in vitro model, knocking down LRP1 could reduce tubular epithelial cell apoptosis and TG accumulation induced by hypoxia-reoxygenation. Our study is the first to demonstrate that LRP1 is involved in tubular epithelial cell injury and TG accumulation in IRI-induced AKI.

LRP1, a type 1 transmembrane protein, is part of the LDL receptor family and plays important role in lipoprotein metabolism. Currently, LRP1 is known to have two primary functions. First, it serves as an endocytic receptor for various ligands on the cell membrane, recognizing and binding to molecules such as VLDL. Second, it acts as a signaling receptor that regulates diverse cellular processes including survival and motility [25]. LRP1 mediates cell injury through activation of the c-Jun N-terminal kinase (JNK) and nuclear factor kappa-B (NF-κB) signaling pathways [26, 27].

Although inhibiting LRP1 could simultaneously improve ischemia-reperfusion-induced AKI and TG accumulation in renal tubular epithelial cells, its protective effect on the kidney may be not due to the antagonism of LRP1-VLDL binding, which leads to TG endocytosis. In our study, exogenously added VLDL increased the TG level in HK-2 cells but had no significant effect on cell viability in vitro, suggesting that TG accumulation may merely be an injury marker of the disease but do not have direct damaging effect. Some studies also found TG, as "inert" lipids, are inherently harmless [28, 29]. In addition, knocking down LRP1 could alleviate tubular epithelial cell apoptosis induced by CCCP without exogenous VLDL. These findings further suggested that the amelioration of RTECs injury by LRP1 antagonism involved mechanisms beyond TG endocytosis. LRP1 mediates the activation of JNK

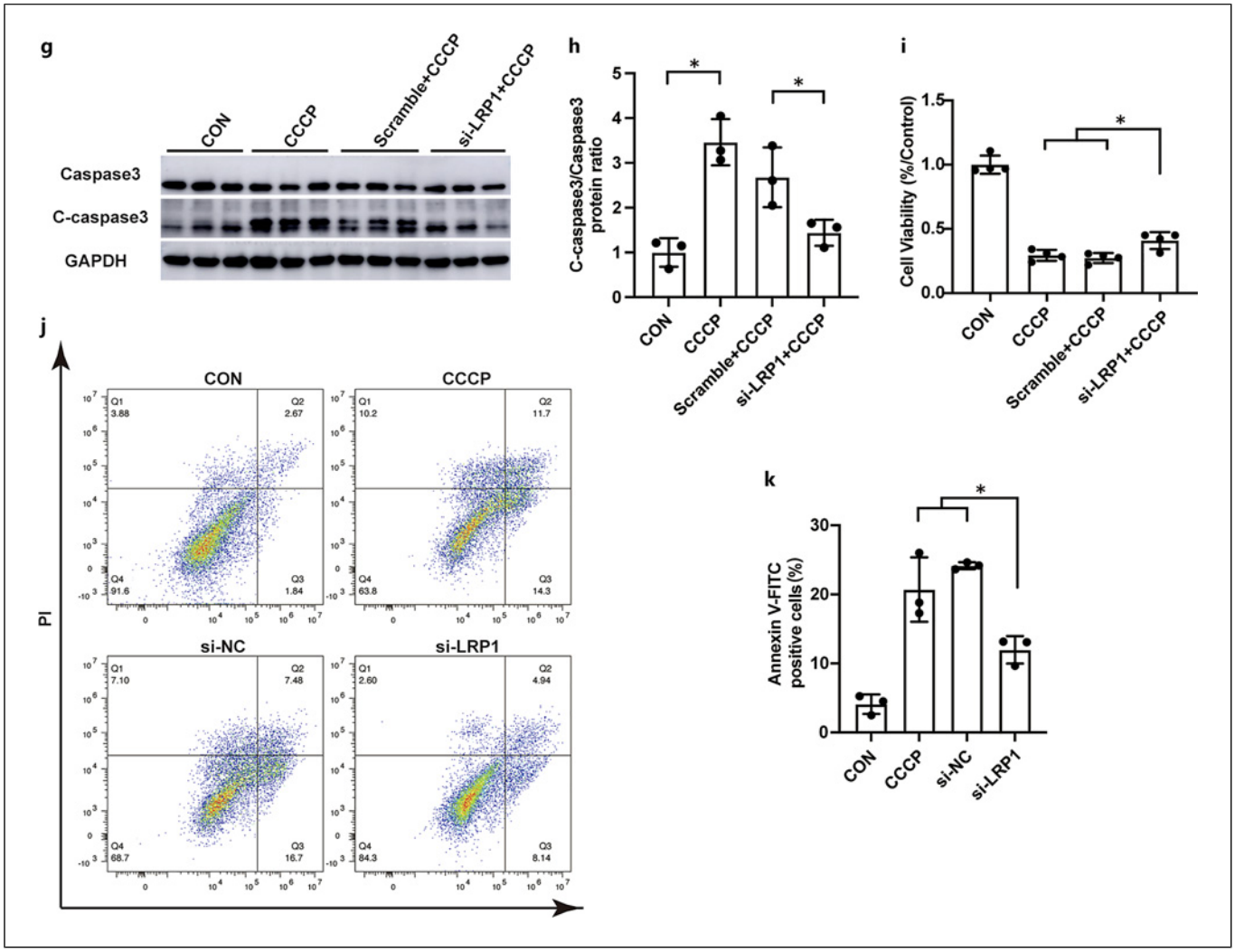

Fig. 4. LRP1-targeted siRNA reduces apoptosis in renal tubular epithelial cell in vitro following CCCP stimulation. HK-2 cells were treated with 15 μM CCCP for 4 h and followed by 2 h reoxygenation. **a** Assessment of cell viability using the CCK-8 assay at varying concentrations of VLDL. **b–d** LRP1-targeted siRNA significantly reduced the mRNA and protein levels of LRP1. Measurement of intracellular TG levels (**e**) and FFA levels (**f**). **g**, **h** Western blot analysis of the expression of C-caspase-3 and caspase-3 in HK-2 cells. **i** Assessment of cell viability using the CCK-8 assay. **j**, **k** Apoptosis was examined by flow cytometry. *$p < 0.05$. CCCP, carbonyl cyanide 3-chlorophenylhydrazone; LRP1, low-density lipoprotein receptor-related protein-1; C-caspase-3, cleaved caspase-3; VLDL, very low-density lipoproteins.

signaling pathway in hepatocytes and exacerbates neuroinflammatory responses by activating the NF-κB signaling pathway in astrocytes during cerebral ischemia [26, 27]. Notably, both JNK and NF-κB signaling pathways contribute to the renal tubular epithelial cell injury in AKI [30, 31].

Although silencing LRP1 could mildly decrease TG levels induced by ATP depletion without exogenous VLDL, this effect of reducing TG was more pronounced in the presence of exogenous VLDL. Therefore, LRP1 may lead to intracellular TG accumulation both by directly affecting TG endocytosis and through other endocytosis-independent effects. According to the current literature, there are no reports indicating that LRP1 affects TG metabolism. We speculate that LRP1 may mediate TG accumulation in tubular epithelial cells through its indirect inhibition of TG metabolism degradation, such as resulting in mitochondrial damage [32].

This study has several limitations. First, the use of RAP in animal experiments may lead to off-target effects. A transgenic model with specific tubular LRP1 knockout would provide more robust evidence to support the

conclusions. Nevertheless, the use of RAP holds promise for future clinical applications. Second, further research is needed to explore the specific mechanism of LRP1's injury effects in AKI in future. In addition, lipid accumulation in renal tubular epithelial cells also contributes to kidney fibrosis following AKI. However, this study focused only on the role of LRP1 during the AKI phase and did not investigate its role in the transition from AKI to chronic kidney disease. Further research is required to determine whether LRP1 contributes to fibrosis and to elucidate the underlying mechanisms.

In conclusion, our study revealed that the upregulated LRP1 on renal tubular epithelial cells is involved in ischemia-reperfusion-induced AKI and TG accumulation. The injury effects of LRP1 on the renal tubules are independent of TG endocytosis. The LRP1 antagonist RAP could alleviate ischemia-reperfusion AKI, providing new therapeutic targets and strategies for future clinical translation.

Statement of Ethics

This study was reviewed and approved by Guangdong Provincial People's Hospital Ethics Review Committee (KY2024-159-01).

Conflict of Interest Statement

The authors have no conflicts of interest to declare.

Funding Sources

This work was financially supported by the National Natural Science Foundation of China (No. 82270712, No. 82070742) and Guangdong-Hong Kong Joint Laboratory on Immunological and Genetic Kidney Diseases (Grant No. 2019B121205005).

Author Contributions

W. Wang: designed the study, performed the experiments, created the figures, and wrote the manuscript. J. Luo and Y. Chen: assisted with the animal experiments. H. Liang, Z. Li, Y. Chen, and J. He: contributed to the in vitro experiments. X. Liang: designed the study, supervised the work, and revised the manuscript. All authors have read and approved the final version of the manuscript.

Data Availability Statement

All data generated or analyzed during this study are included in this article and its supplementary material file. Further inquiries can be directed to the corresponding author.

References

1 Susantitaphong P, Cruz DN, Cerda J, Abulfaraj M, Alqahtani F, Koulouridis I, et al. World incidence of AKI: a meta-analysis. Clin J Am Soc Nephrol. 2013;8(9):1482–93. https://doi.org/10.2215/CJN.00710113

2 Noh MR, Padanilam BJ. Cell death induced by acute renal injury: a perspective on the contributions of accidental and programmed cell death. Am J Physiol Ren Physiol. 2024;327(1):F4–20. https://doi.org/10.1152/ajprenal.00275.2023

3 Yao W, Chen Y, Li Z, Ji J, You A, Jin S, et al. Single cell RNA sequencing identifies a unique inflammatory macrophage subset as a druggable target for alleviating acute kidney injury. Adv Sci. 2022;9(12):2103675. https://doi.org/10.1002/advs.202103675

4 Basile DP. The endothelial cell in ischemic acute kidney injury: implications for acute and chronic function. Kidney Int. 2007;72(2):151–6. https://doi.org/10.1038/sj.ki.5002312

5 Martín-Saiz L, Guerrero-Mauvecin J, Martín-Sanchez D, Fresnedo O, Gómez MJ, Carrasco S, et al. Ferrostatin-1 modulates dysregulated kidney lipids in acute kidney injury. J Pathol. 2022;257(3):285–99. https://doi.org/10.1002/path.5882

6 Moreno-Gordaliza E, Marazuela MD, Pastor Ó, Lázaro A, Gómez-Gómez MM. Lipidomics reveals cisplatin-induced renal lipid alterations during acute kidney injury and their attenuation by cilastatin. Int J Mol Sci. 2021;22(22):12521. https://doi.org/10.3390/ijms222212521

7 Sears SM, Dupre TV, Shah PP, Davis DL, Doll MA, Sharp CN, et al. Neutral ceramidase deficiency protects against cisplatin-induced acute kidney injury. J Lipid Res. 2022;63(3):100179. https://doi.org/10.1016/j.jlr.2022.100179

8 AbouRjaili G, Shtaynberg N, Wetz R, Costantino T, Abela GS. Current concepts in triglyceride metabolism, pathophysiology, and treatment. Metabolism. 2010;59(8):1210–20. https://doi.org/10.1016/j.metabol.2009.11.014

9 Chait A, Ginsberg HN, Vaisar T, Heinecke JW, Goldberg IJ, Bornfeldt KE. Remnants of the triglyceride-rich lipoproteins, diabetes, and cardiovascular disease. Diabetes. 2020;69(4):508–16. https://doi.org/10.2337/dbi19-0007

10 Khan S, Cabral PD, Schilling WP, Schmidt ZW, Uddin AN, Gingras A, et al. Kidney proximal tubule lipoapoptosis is regulated by fatty acid transporter-2 (FATP2). J Am Soc Nephrol. 2018;29(1):81–91. https://doi.org/10.1681/ASN.2017030314

11 Li S, Nagothu K, Ranganathan G, Ali SM, Shank B, Gokden N, et al. Reduced kidney lipoprotein lipase and renal tubule triglyceride accumulation in cisplatin-mediated acute kidney injury. Am J Physiol Ren Physiol. 2012;303(3):F437–48. https://doi.org/10.1152/ajprenal.00111.2012

12 Zager RA, Johnson ACM, Hanson SY. Renal tubular triglyercide accumulation following endotoxic, toxic, and ischemic injury. Kidney Int. 2005;67(1):111–21. https://doi.org/10.1111/j.1523-1755.2005.00061.x

13 Johnson ACM, Stahl A, Zager RA. Triglyceride accumulation in injured renal tubular cells: alterations in both synthetic and catabolic pathways. Kidney Int. 2005;67(6):2196–209. https://doi.org/10.1111/j.1523-1755.2005.00325.x

14 Actis Dato V, Chiabrando GA. The role of low-density lipoprotein receptor-related protein 1 in lipid metabolism, glucose homeostasis and inflammation. Int J Mol Sci. 2018;19(6):1780. https://doi.org/10.3390/ijms19061780

15 Beisiegel U, Weber W, Ihrke G, Herz J, Stanley KK. The LDL-receptor-related protein, LRP, is an apolipoprotein E-binding protein. Nature. 1989;341(6238):162–4. https://doi.org/10.1038/341162a0
16 Lillis AP, Van Duyn LB, Murphy-Ullrich JE, Strickland DK. LDL receptor-related protein 1: unique tissue-specific functions revealed by selective gene knockout studies. Physiol Rev. 2008;88(3):887–918. https://doi.org/10.1152/physrev.00033.2007
17 Xie Z, Dong W, Zhang L, Wang M, Xiao Z, Zhang Y, et al. NFAT inhibitor 11R-VIVIT ameliorates mouse renal fibrosis after ischemia-reperfusion-induced acute kidney injury. Acta Pharmacol Sin. 2022;43(8):2081–93. https://doi.org/10.1038/s41401-021-00833-y
18 Prasad JM, Migliorini M, Galisteo R, Strickland DK. Generation of a potent low density lipoprotein receptor-related protein 1 (LRP1) antagonist by engineering a stable form of the receptor-associated protein (RAP) D3 domain. J Biol Chem. 2015;290(28):17262–8. https://doi.org/10.1074/jbc.M115.660084
19 Brooks C, Wei Q, Cho S-G, Dong Z. Regulation of mitochondrial dynamics in acute kidney injury in cell culture and rodent models. J Clin Investig. 2009;119(5):1275–85. https://doi.org/10.1172/JCI37829
20 Mikhailov V, Mikhailova M, Pulkrabek DJ, Dong Z, Venkatachalam MA, Saikumar P. Bcl-2 prevents bax oligomerization in the mitochondrial outer membrane. J Biol Chem. 2001;276(21):18361–74. https://doi.org/10.1074/jbc.M100655200
21 Wang H, Eckel RH. Lipoprotein lipase: from gene to obesity. Am J Physiol Endocrinol Metab. 2009;297(2):E271–88. https://doi.org/10.1152/ajpendo.90920.2008
22 Bu G, Schwartz AL. RAP, a novel type of ER chaperone. Trends Cell Biol. 1998;8(7):272–6. https://doi.org/10.1016/s0962-8924(98)01283-5
23 Reid KM, Brown GC. LRPAP1 is released from activated microglia and inhibits microglial phagocytosis and amyloid beta aggregation. Front Immunol. 2023;14:1286474. https://doi.org/10.3389/fimmu.2023.1286474
24 May P, Herz J, Bock HH. Molecular mechanisms of lipoprotein receptor signalling. Cell Mol Life Sci. 2005;62(19–20):2325–38. https://doi.org/10.1007/s00018-005-5231-z
25 Lin L, Hu K. LRP-1: functions, signaling and implications in kidney and other diseases. Int J Mol Sci. 2014;15(12):22887–901. https://doi.org/10.3390/ijms151222887
26 Wang L, Shen F, Zhang M, He Q, Zhao H, Yu X, et al. Cytotoxicity mechanism of α-MMC in normal liver cells through LRP1 mediated endocytosis and JNK activation. Toxicology. 2016;357–358:33–43. https://doi.org/10.1016/j.tox.2016.05.025
27 Zhang X, Polavarapu R, She H, Mao Z, Yepes M. Tissue-type plasminogen activator and the low-density lipoprotein receptor-related protein mediate cerebral ischemia-induced nuclear factor-kappaB pathway activation. Am J Pathol. 2007;171(4):1281–90. https://doi.org/10.2353/ajpath.2007.070472
28 Listenberger LL, Han X, Lewis SE, Cases S, Farese RV, Ory DS, et al. Triglyceride accumulation protects against fatty acid-induced lipotoxicity. Proc Natl Acad Sci USA. 2003;100(6):3077–82. https://doi.org/10.1073/pnas.0630588100
29 Weinberg JM. Lipotoxicity. Kidney Int. 2006;70(9):1560–6. https://doi.org/10.1038/sj.ki.5001834
30 Luo F, Shi J, Shi Q, Xu X, Xia Y, He X. Mitogen-activated protein kinases and hypoxic/ischemic nephropathy. Cell Physiol Biochem. 2016;39(3):1051–67. https://doi.org/10.1159/000447812
31 Li Z-L, Ji J-L, Wen Y, Cao J-Y, Kharbuja N, Ni W-J, et al. HIF-1α is transcriptionally regulated by NF-κB in acute kidney injury. Am J Physiol Ren Physiol. 2021;321(2):F225–35. https://doi.org/10.1152/ajprenal.00119.2021
32 Velmurugan GV, Hubbard WB, Prajapati P, Vekaria HJ, Patel SP, Rabchevsky AG, et al. LRP1 deficiency promotes mitostasis in response to oxidative stress: implications for mitochondrial targeting after traumatic brain injury. Cells. 2023;12(10):1445. https://doi.org/10.3390/cells12101445